Journal of The Electrochemical Society, **153** (11) A2030-A2035 (2006)
0013-4651/2006/153(11)/A2030/6/$20.00 © The Electrochemical Society

Thermal Stability of the $Li(Ni_{0.8}Co_{0.15}Al_{0.05})O_2$ Cathode in the Presence of Cell Components

I. Belharouak,* D. Vissers,* and K. Amine*,z

Argonne National Laboratory, Chemical Engineering Division, Argonne, Illinois 60439, USA

The $Li(Ni_{0.8}Co_{0.15}Al_{0.05})O_2$ cathode, a potential candidate for hybrid electric vehicle applications, has been electrochemically charged in powder form without a carbon additive and binder. The thermal stability of the resulting $Li_{0.53}(Ni_{0.8}Co_{0.15}Al_{0.05})O_2$ powder was studied by thermal gravimetric analysis (TGA), gas chromatography/mass spectrometry, and X-ray diffraction techniques under different gas flows. The transformation of $Li_{0.53}(Ni_{0.8}Co_{0.15}Al_{0.05})O_2$-layered material to the NiO-type structure material and/or to nickel metal was correlated to the oxidizing/reducing properties of the TGA gas flow under which the thermal decomposition of the $Li_{0.53}(Ni_{0.8}Co_{0.15}Al_{0.05})O_2$ occurred. Differential scanning calorimetry measurements were performed on $Li_{0.53}(Ni_{0.8}Co_{0.15}Al_{0.05})O_2$ powder in the presence of solvent, salt, or binder independently. The reactivity at 170°C between $Li_{0.53}(Ni_{0.8}Co_{0.15}Al_{0.05})O_2$ and ethylene carbonate (EC) solvent was found to be dependent on the $Li_{0.53}(Ni_{0.8}Co_{0.15}Al_{0.05})O_2$ oxide/EC weight ratio. The exothermic reaction observed in the presence of other solvents was not greatly affected, as long as the oxide/solvent weight ratios were kept very close to one another. The $LiPF_6$ salt, when added to the charged oxide powder, was found to shift the exothermic reaction to 220°C when it was dissolved in the electrolyte and 270°C when it was added in the solid form. When polyvinylidene fluoride binder was added to $Li_{0.53}(Ni_{0.8}Co_{0.15}Al_{0.05})O_2$ powder, the exothermic reaction occurred at high temperatures (340°C). The initiation of the exothermic reaction has been primarily attributed to the oxidation of the electrolyte by the oxygen gas released from $Li_{0.53}(Ni_{0.8}Co_{0.15}Al_{0.05})O_2$ after the collapse of its layered structure.
 [DOI: 10.1149/1.2336994]

Manuscript submitted February 27, 2006; revised manuscript received May 17, 2006. Available electronically September 6, 2006.

Despite the introduction of lithium-ion batteries in a wide range of consumer electronics applications, there are still some safety concerns, mainly associated with the potential use of these batteries in large-scale applications such as hybrid electric vehicles (HEVs).[1] In the past five years, Argonne National Laboratory (ANL) has been primarily working on understanding the power fade mechanisms of high-power 18650 cells that incorporate $Li(Ni_{0.8}Co_{0.15}Al_{0.05})O_2$ as the positive electrode, graphite as the negative electrode, and 1.2 M $LiPF_6$ [ethylene carbonate (EC)/ethyl methyl carbonate (EMC) = 3:7 wt %] as the electrolyte.[2,3] A second goal of this project is to conduct detailed thermal characterization studies on each cell component to understand the mechanisms responsible for the thermal abuse of these cells.

Most of the previous safety studies have concentrated on performing differential scanning calorimetry (DSC) and accelerated rate calorimetry (ARC) experiments on the positive and negative electrodes in the presence of electrolytes.[4-7] Our approach has focused instead on investigating the thermal stability of every single-cell component and their interactions, in order to come up with a better understanding of the thermal behavior of the cell. The aim of the present work is to evaluate the safety characteristics of the $Li(Ni_{0.8}Co_{0.15}Al_{0.05})O_2$ powder in its charged state and to investigate the thermal degradation of this positive material in the presence of cell components. To this end, the $Li(Ni_{0.8}Co_{0.15}Al_{0.05})O_2$ oxide powder was electrochemically charged to 4.2 V without adding binder or carbon additive. In the first step, the resulting $Li_{0.53}(Ni_{0.8}Co_{0.15}Al_{0.05})O_2$ powder was studied by thermal gravimetric analysis (TGA) coupled with gas chromatography/mass spectrometry (GC/MS). In the second step, the thermal behavior of $Li_{0.53}(Ni_{0.8}Co_{0.15}Al_{0.05})O_2$ was investigated in the presence of several organic solvents by DSC and X-ray diffraction (XRD) techniques. Furthermore, the thermal effects of the $LiPF_6$ salt powder and the polyvinylidene fluoride (PVDF) binder were also investigated in the presence of $Li_{0.53}(Ni_{0.8}Co_{0.15}Al_{0.05})O_2$.

Experimental

The layered structure of $Li(Ni_{0.8}Co_{0.15}Al_{0.05})O_2$, received from Fuji Chemical Corporation, was determined by XRD, and its composition was confirmed by the inductively coupled plasma (ICP) analysis.

The positive electrode in this study was made by pressing $Li(Ni_{0.8}Co_{0.15}Al_{0.05})O_2$ powder between two layers of stainless steel mesh to form a 100 μm thin electrode. This technique allowed us to charge this powder without adding carbon and PVDF binder additives because it provided a sort of electronic network for the material in addition to its role of holding the powder in a mechanically stable layer. Several cells were then fabricated with this electrode vs metallic lithium in the presence of the 1.2 M $LiPF_6$ (EC/EMC = 3:7 wt %) electrolyte. These cells were assembled inside a helium-filled dry box using coin-type containers (CR2032: 1.6 cm^2). The charge/discharge measurements were carried out at room temperature in a potential range between 3.0 and 4.2 V at the current density of 15 mA/g. After a formation cycle, the $Li/Li(Ni_{0.8}Co_{0.15}Al_{0.05})O_2$ cells were charged to 4.2 V and kept at this potential for 3 h. Thereafter, the charged active powders were recovered inside a helium-filled dry box and rinsed with dimethyl carbonate (DMC) and acetone. The powders were then dried under vacuum at 60°C for several hours.

TGA experiments were conducted on the $Li_{0.53}(Ni_{0.8}Co_{0.15}Al_{0.05})O_2$ powder (typically 20 mg inside a platinum pan). The data were collected using a Seiko Exstar 6000 instrument at a scan rate of 5°C/min in the temperature range of 30–700°C. The TGA experiments were performed under either a flow of purified air, nitrogen, or a nitrogen/hydrogen mixture (4 wt %). The reference pan of the furnace consisted of an empty platinum pan. The gas collection and analyses were carried out using a Hewlett-Packard 6890 GC system and a Hewlett-Packard 5973 mass selective detector, which is a GC/MS instrument. In this case, the GC/MS instrument was connected to the TGA apparatus in order to investigate the oxygen released from the charged $Li(Ni_{0.8}Co_{0.15}Al_{0.05})O_2$ powder during the TGA thermal decomposition between 25 and 600°C. The TGA instrument outlet was attached to the GC/MS instrument inlet using a stainless steel pipe engineered for this purpose. The GC/MS apparatus was calibrated using standard gases.

DSC experiments were conducted on the above active powder using a Perkin–Elmer Pyris 1 instrument. Typically, 3 mg of a

* Electrochemical Society Active Member.
z E-mail: amine@cmt.anl.gov

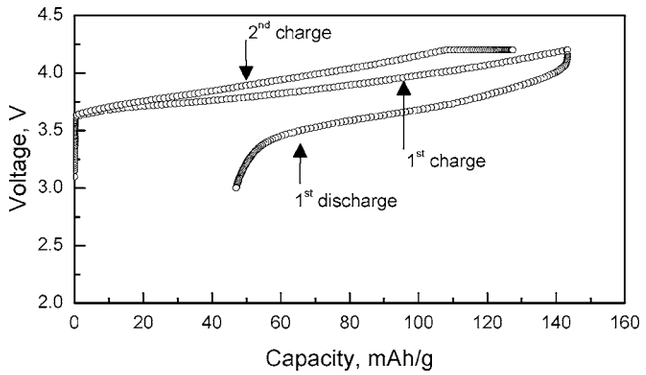

Figure 1. Electrochemical charge/discharge/charge profile of a $Li/Li(Ni_{0.8}Co_{0.15}Al_{0.05})O_2$ powder cell.

charged $Li_{0.53}(Ni_{0.8}Co_{0.15}Al_{0.05})O_2$ powder and 3 μL of a solvent or electrolyte were hermetically sealed inside stainless steel high-pressure capsules to prevent leakage of the solvents. The DSC curves were recorded between 30 and 375°C at a scan rate of 10°C/min. An empty stainless steel capsule was used as a reference pan. The reproducibility of the DSC data was ensured by recording multiple samples for each experiment. Note that the calculated heats from the DSC curves are expressed in the text with the unit (J/g); (g) refers to the weight of the $Li_{0.53}(Ni_{0.8}Co_{0.15}Al_{0.05})O_2$ powder unless otherwise specified.

Powder XRD patterns of the samples were recorded on a Siemens D5000 powder diffractometer using Cu Kα radiation in the angular range of 10–80° (2θ) with a 0.02° (2θ) step. The unit cell parameters were calculated using a Rietveld profile matching refinement of the XRD diagrams.[8]

Results

Figure 1 shows the charge/discharge profile of a $Li/Li(Ni_{0.8}Co_{0.15}Al_{0.05})O_2$ cell at C/10 rate. In this case, the cell polarization between the charge and discharge was high because no carbon conductive additive was added during the process of making the positive electrode. The capacity of the cell after being charged to 4.2 V was 120 mAh/g, which is equivalent to almost 50% lithium removal from the $Li(Ni_{0.8}Co_{0.15}Al_{0.05})O_2$ material. The chemical composition of the charged $Li(Ni_{0.8}Co_{0.15}Al_{0.05})O_2$ powder was analyzed by the ICP technique and was determined to be about $Li_{0.53}(Ni_{0.8}Co_{0.15}Al_{0.05})O_2$.

Figure 2 shows the XRD patterns of the $Li(Ni_{0.8}Co_{0.15}Al_{0.05})O_2$ powder and $Li_{0.53}(Ni_{0.8}Co_{0.15}Al_{0.05})O_2$ charged powder. In both cases, the diffraction lines can be indexed according to the $R\bar{3}m$ space group of the α-$NaFeO_2$ structural model. The hexagonal lattice parameters for these oxides are: [a = 2.852(4) Å, c = 14.235(5) Å] and [a = 2.824(7) Å, c = 14.403(5) Å], respectively. In this case, an expansion of the c parameter was observed for $Li_{0.53}(Ni_{0.8}Co_{0.15}Al_{0.05})O_2$ when compared to the initial fully lithiated phase.

Figure 3 shows the TGA curves of the $Li_{0.53}(Ni_{0.8}Co_{0.15}Al_{0.05})O_2$ powder carried out under different atmospheres and the XRD patterns of the powders recovered after each TGA experiment. Under air flow, a 10 wt % weight loss associated with the thermal degradation of $Li_{0.53}(Ni_{0.8}Co_{0.15}Al_{0.05})O_2$ occurred between 200 and 420°C (Fig. 3a). The XRD diagram of the material recovered at the end of the TGA experiment is characteristic of a NiO-type structure,[9] due to the partial oxygen release from the charged powder (Fig. 3d). In the same figure, we also noticed a weak (003) diffraction line, which is characteristic of a remaining layered $Li_{0.53}(Ni_{0.8}Co_{0.15}Al_{0.05})O_2$ that was not decomposed. Under a N_2 flow, the TGA/XRD results showed similar trends in comparison

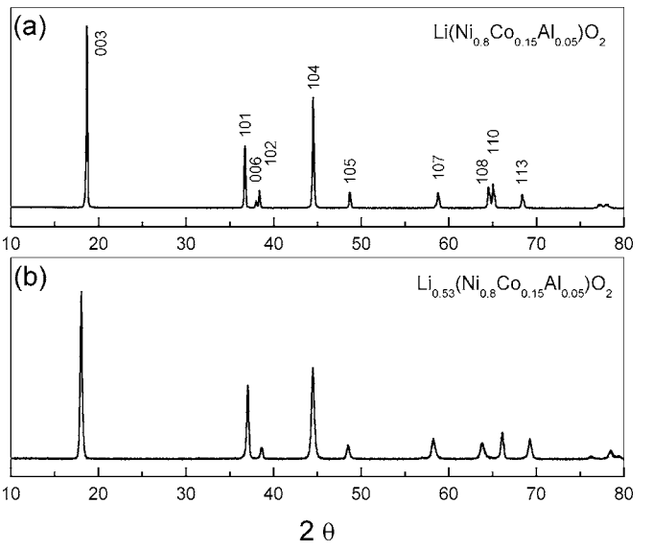

Figure 2. XRD patterns recorded for (a) pristine $Li(Ni_{0.8}Co_{0.15}Al_{0.05})O_2$ and (b) $Li_{0.53}(Ni_{0.8}Co_{0.15}Al_{0.05})O_2$ obtained after an electrochemical charge at 4.2 V.

with the experiment conducted under the air flow (Fig. 3b and e). However, the material exposed to a mix of N_2/H_2 (4 wt %) exhibited a different thermal behavior. In fact, under this reducing atmosphere, the material lost around 11 wt % of its initial weight between 200 and 280°C to form a NiO-type compound and an additional 21 wt % between 280 and 600°C to give rise to a metallic nickel-type compound[10] (Fig. 3c and f). In this case, the 32 wt % weight loss took place after all oxygen atoms were released from the $Li_{0.53}(Ni_{0.8}Co_{0.15}Al_{0.05})O_2$ powder leading to a metallic nickel-type compound.

Figure 4 shows the in situ gas analysis during the TGA experiment that was conducted on the $Li_{0.53}(Ni_{0.8}Co_{0.15}Al_{0.05})O_2$ powder between 25 and 700°C under a high-purity N_2 flow. The gas detected by the GC/MS during the weight loss is assigned to the oxygen released from $Li_{0.53}(Ni_{0.8}Co_{0.15}Al_{0.05})O_2$ during its thermal de-

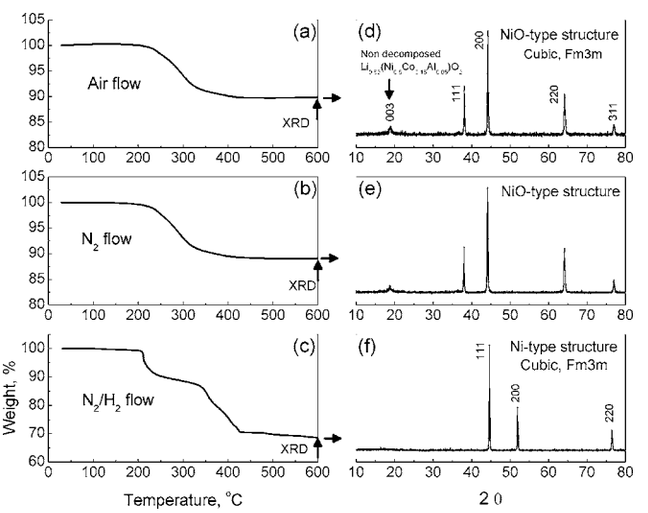

Figure 3. TGA curves of the $Li_{0.53}(Ni_{0.8}Co_{0.15}Al_{0.05})O_2$ charged powder under different atmospheres: (a) under air flow, (b) under N_2 flow, and (c) under N_2/H_2 flow. The corresponding XRD patterns (d), (e), and (f), respectively, were recorded on the recovered powders at the end of each TGA experiment.

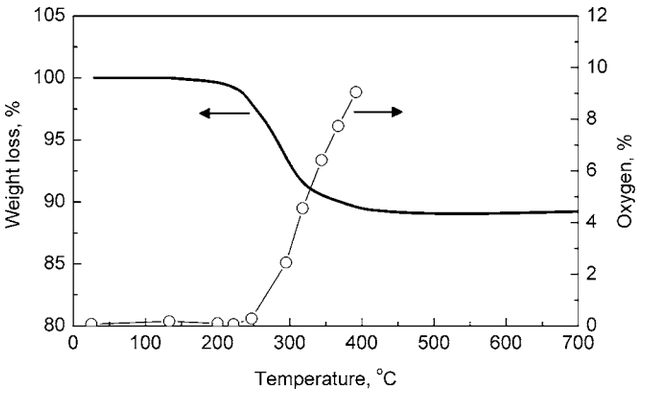

Figure 4. TGA experiment coupled with gas analysis of $Li_{0.53}(Ni_{0.8}Co_{0.15}Al_{0.05})O_2$ powder.

composition, as reported by Guilmard et al.[11-13] A preliminary baseline test confirmed that no oxygen was detected when the TGA experiment was carried out without the presence of the active powder.

To study the reactivity between the $Li_{0.53}(Ni_{0.8}Co_{0.15}Al_{0.05})O_2$ powder and other cell components, we first investigated the reactivity of different solvents such as EC, EMC, and propylene carbonate (PC) with $Li_{0.53}(Ni_{0.8}Co_{0.15}Al_{0.05})O_2$ powder. In our approach, we assumed that the reactivity between $Li_{0.53}(Ni_{0.8}Co_{0.15}Al_{0.05})O_2$ and a solvent can be viewed as a simple oxidation reaction between the solvent and the O_2 gas released from the charged active powder. Note that pure solvents alone do not generate heat during thermal analysis experiments, as reported by MacNeil et al.[14] In the case of the EC solvent, the reaction can be written as follows

$$C_3H_4O_3(g) + 2.5O_2(g) \rightarrow 2H_2O(g) + 3CO_2(g)[\text{g stands for gas}] \quad [1]$$

The amount of heat generated from the above oxidation reaction depends on the ratio of $Li_{0.53}(Ni_{0.8}Co_{0.15}Al_{0.05})O_2$ oxide to EC solvent. Figure 5 shows the DSC measurements obtained for different $Li_{0.53}(Ni_{0.8}Co_{0.15}Al_{0.05})O_2$/EC weight ratios and the XRD patterns of the obtained material at the end of the DSC experiments. In these figures, the endothermic peak observed at 45°C corresponds to the melting of the EC solvent from a solid to a liquid. From the DSC curves, up to three exothermic peaks can be observed, depending on the $Li_{0.53}(Ni_{0.8}Co_{0.15}Al_{0.05})O_2$/EC weight ratio. In the case of a small amount of EC solvent (4 wt %), only two peaks (α and γ) are observed at 210 and 245°C (Fig. 5a). When the amount of the EC solvent increases to 22 wt %, a third exothermic peak, labeled β, around 225°C is detected between the α and γ peaks. In all cases, the onset temperature of the initial thermal peak was 170°C regardless of the oxide/EC weight ratio. The total heat associated with the appearance of these peaks ranged from 725 to 1150 J/g and was correlated with the amount of the EC solvent. For instance, when the amount of EC is small, the heat associated with the exothermic reaction is also small (725 J/g). Therefore, we expect that a maximum heat can be generated in situations where all released O_2 from the cathode can be consumed by the solvent.

The XRD diagrams show the structure of the obtained powder at the end of the DSC experiments (Fig. 5c and d). It is clear from these results that the EC solvent reduced the $Li_{0.53}(Ni_{0.8}Co_{0.15}Al_{0.05})O_2$ powder, starting from 170°C, leading to a partial oxygen release, and thus to a structural change from a layered to a NiO-type structure. The oxygen released then oxidized the solvent, leading to the exothermic heat measured by DSC. Furthermore, the appearance of the (111) diffraction line in Fig. 5d indicates the presence of nickel metal. This peak appears only when a large amount of EC is used, which could further reduce the active oxide, leading to the appearance of metallic nickel.

Figure 6 shows the DSC curves obtained using 22 wt % of EC solvent, as in the case of Fig. 5b. In this case, the structural change of the oxide was investigated before the initial thermal heat (180°C) (Fig. 6a), in the middle of the thermal heat (250°C) (Fig. 6b), and at the end of the DSC experiment (375°C) (Fig. 6c). At 180°C, the layered structure of $Li_{0.53}(Ni_{0.8}Co_{0.15}Al_{0.05})O_2$ remained intact, as can be noticed in the XRD pattern recorded on the sample after the DSC experiment (Fig. 6d). In the middle of the reaction (250°C), the material transformed mostly to a NiO-type compound with a very small amount of unreacted $Li_{0.53}(Ni_{0.8}Co_{0.15}Al_{0.05})O_2$, as indicated by the (003) diffraction line shown in (Fig. 6e). At the end of the reaction (375°C), the powder completely converted to a NiO-type material with the presence of a nickel-based compound.

To further corroborate our results observed in the case of the EC solvent, we investigated other solvents such as EMC and PC. Figures 7a and b shows the DSC measurements performed on the $Li_{0.53}(Ni_{0.8}Co_{0.15}Al_{0.05})O_2$ powder in the presence of EMC and PC solvents, respectively. The oxide/solvent weight ratios are also

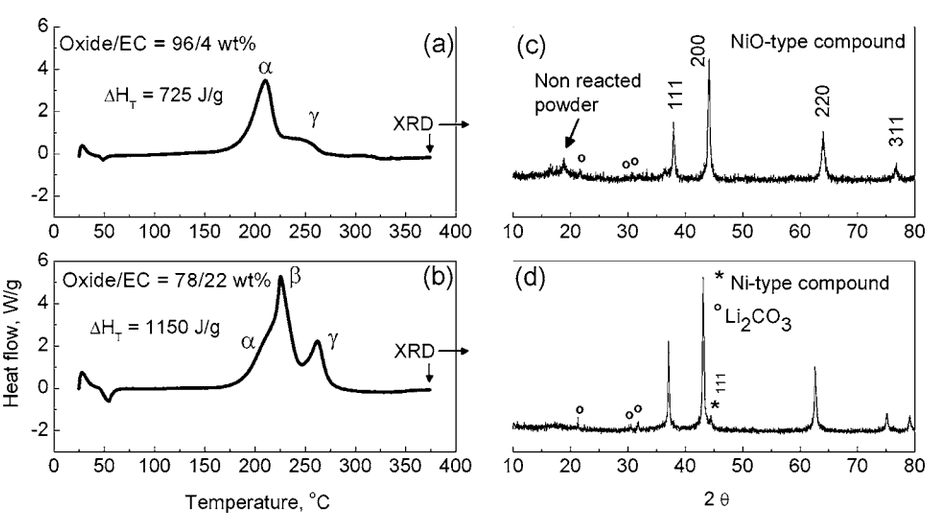

Figure 5. DSC profiles of $Li_{0.53}(Ni_{0.8}Co_{0.15}Al_{0.05})O_2$/EC mixtures. The XRD patterns were recorded, after the DSC experiments, on the recuperated powders for every oxide/EC weight ratio.

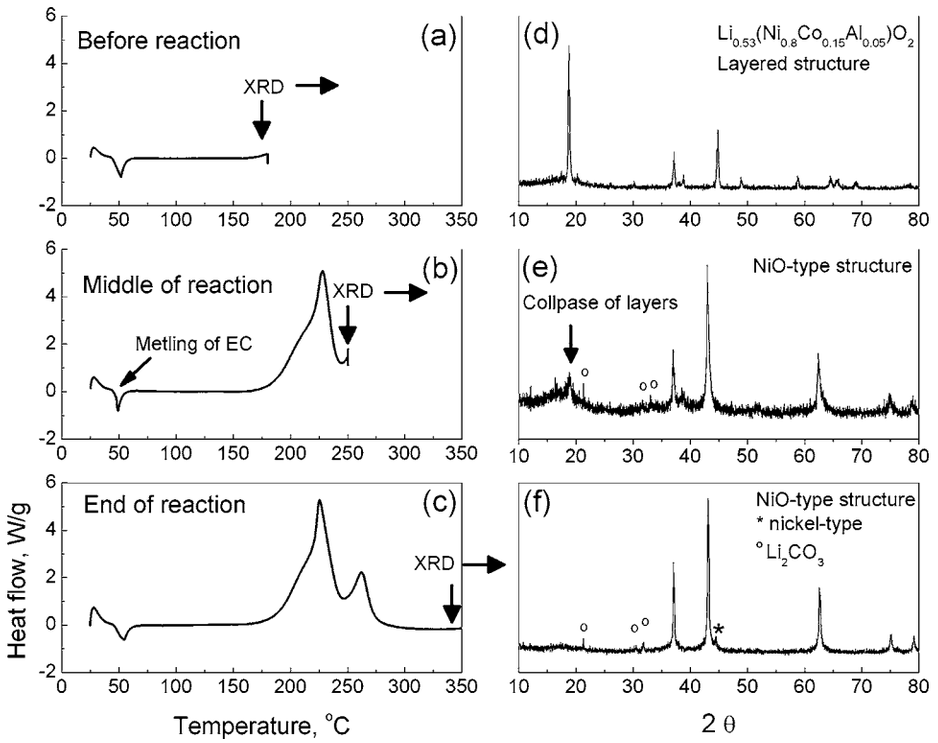

Figure 6. Thermal degradation of $Li_{0.53}(Ni_{0.8}Co_{0.15}Al_{0.05})O_2$ in the presence of EC solvent. XRD diagrams show a structural comparison before, in the middle of, and after the exothermic reaction that occurred between the $Li_{0.53}(Ni_{0.8}Co_{0.15}Al_{0.05})O_2$ powder and the EC solvent.

shown in these figures, as well as the total heat associated with the observed exothermic reactions. Because the oxide solvent ratios were the same in the EMC (Fig. 7a) and PC (Fig. 7b) cases, the amount of the heat generated in both cases was almost the same (1060 J/g for EMC and 1030 J/g for PC). This result clearly shows that the oxidation of the solvent by the oxygen released from the oxide is responsible for the observed thermal heat regardless of the nature of the solvent used in the electrolyte.

Figure 8 shows the DSC curve of the $LiPF_6$ salt only (Fig. 8a), the DSC curve of the $Li_{0.53}(Ni_{0.8}Co_{0.15}Al_{0.05})O_2$ oxide mixed with the $LiPF_6$ salt (Fig. 8b), and the XRD pattern of the sample recovered at the end of the DSC experiment with the $Li_{0.53}(Ni_{0.8}Co_{0.15}Al_{0.05})O_2$ oxide mixed with the $LiPF_6$ salt (Fig. 8c).

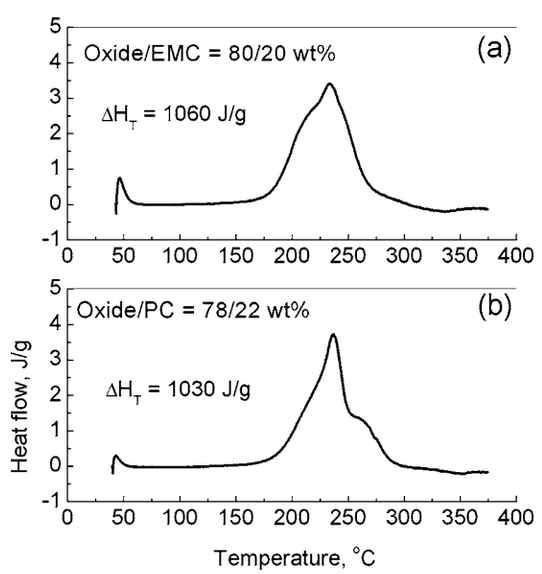

Figure 7. DSC profiles of the $Li_{0.53}(Ni_{0.8}Co_{0.15}Al_{0.05})O_2$ powder in the presence of the EMC and PC solvents.

$LiPF_6$ salt is known to reversibly decompose according to the following reaction[15]

$$LiPF_6(s) \leftrightarrows LiF(s) + PF_5(g) \quad [2]$$

In our case, $LiPF_6$ salt was found to have a melting point at 195°C with a broad decomposition peak covering the temperature range of 240–310°C (Fig. 8a). When $LiPF_6$ solid was mixed with the $Li_{0.53}(Ni_{0.8}Co_{0.15}Al_{0.05})O_2$ powder (oxide/salt ratio = 72/28), at least four peaks were observed in the DSC curve, as shown in Fig. 8b. The low-temperature endothermic peak at 195°C was attributed to the $LiPF_6$ melting point, by analogy with the plot in Fig. 8a. The three other exothermic peaks have maximums at 286, 305, and 325°C, with an onset temperature at 270°C. The total heat associated with the appearance of these three peaks was very small, around 380 J/g. As mentioned above, the unstable $LiPF_6$ salt decomposes, starting from 240°C, to form LiF solid and PF_5 in a gaseous state. LiF is very stable within the temperature range of the DSC experiment and is expected to be inactive in the presence of the $Li_{0.53}(Ni_{0.8}Co_{0.15}Al_{0.05})O_2$ powder. However, PF_5 is a very reactive gas, so it could be responsible for the initiation of an exothermic reaction with the charged oxide powder. No exothermic reaction was detected before 240°C, which is the starting temperature of the decomposition of $LiPF_6$. Figure 8c shows the XRD pattern of the material recovered at the end of the DSC experiment. This figure shows that $Li_{0.53}(Ni_{0.8}Co_{0.15}Al_{0.05})O_2$ converted to a NiO-type compound with the presence of LiF, the remaining nonreacted oxide material, and other diffraction lines that could not be indexed at the moment. This result indicates that $PF_5(g)$ acted as a reducing agent in the presence of the layered $Li_{0.53}(Ni_{0.8}Co_{0.15}Al_{0.05})O_2$ material. The latter transformed to a NiO-type compound by a mechanism that involved an exothermic reaction, apparently between the released oxygen and $PF_5(g)$. This reaction generates very limited heat, even though we used a large excess of salt; therefore, the contribution of the salt to the overall heat observed in a cell is expected to be minor.

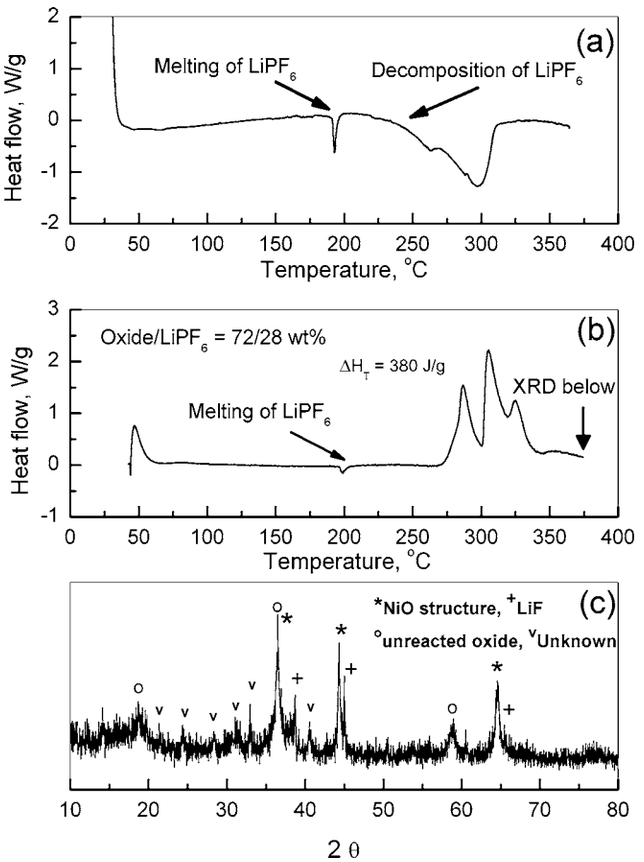

Figure 8. DSC profiles of (a) $LiPF_6$ salt and (b) $Li_{0.53}(Ni_{0.8}Co_{0.15}Al_{0.05})O_2$ and $LiPF_6$ together. Figure 8c shows the XRD diagram obtained for the recuperated oxide sample after the DSC measurement.

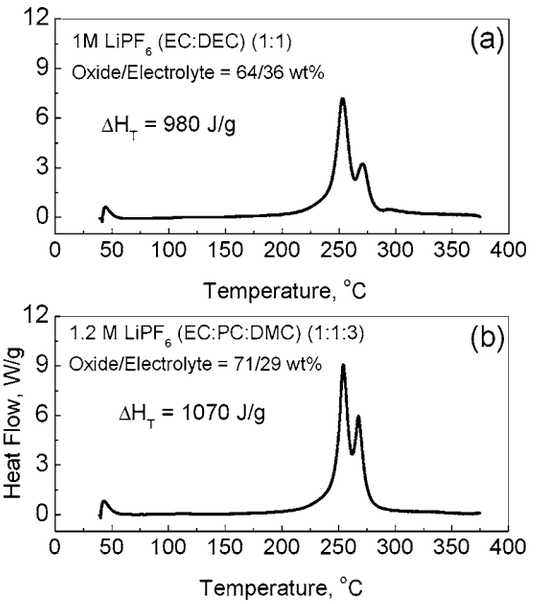

Figure 9. DSC profiles of the $Li_{0.53}(Ni_{0.8}Co_{0.15}Al_{0.05})O_2$ powder in the presence of different electrolytes.

Figure 9 shows the DSC results of $Li_{0.53}(Ni_{0.8}Co_{0.15}Al_{0.05})O_2$ in the presence of (a) 1 M $LiPF_6$ (EC/DEC = 1:1 wt %) electrolyte (Fig. 9a) or (b) 1.2 M $LiPF_6$ (EC/PC/DMC = 1:1:3 wt %) electrolyte (Fig. 9b). The oxide/electrolyte weight ratios were kept as close as possible, as shown in these figures. Under these conditions, it seems that the $Li_{0.53}(Ni_{0.8}Co_{0.15}Al_{0.05})O_2$ powder reacted in a quite similar way, resulting in similar heat generation regardless of the nature of the electrolyte. Basically, two exothermic peaks were observed at 253 and 268°C with an onset temperature at 220°C. The generated heats were 980 and 1070 J/g for the reactions that involved (a) and (b) electrolytes, respectively. From all these data, one can notice that the onset temperature (220°C) recorded in the case of the oxide/electrolyte reaction was between the onset temperatures of the oxide/solvent (170°C) and the oxide/salt reaction (270°C). In the presence of an electrolyte, the reaction of the charged powder tends to shift toward higher temperature, probably because of the flame-retardant characteristics of the salt, as reported earlier by MacNeil et al.[16]

Figure 10 shows the DSC result of the $Li_{0.53}(Ni_{0.8}Co_{0.15}Al_{0.05})O_2$ charged powder mixed with 26 wt % of PVFD $[CH_2 - CF_2]_n$ solid. In this case, the melting point of PVDF was detected between 160 and 170°C. In the first step, we ran a DSC scan on PVDF solid alone (result not shown here), but no noticeable heat was measured in the temperature range of 25–375°C. When the binder was added to the charged powder, a small exothermic reaction was observed at 350°C with an onset temperature at 340°C. The total heat associated with this reaction was 470 J/g. In a real cell design, the amount of PVDF does not exceed 8 wt %; therefore, we should expect much lower heat than the one observed in this study (26 wt %). By the end of the DSC experiment, the remaining sample was checked by XRD (Fig. 10b). Two predominant phases were indexed in the XRD diagram: NiO-type compound and LiF. These compounds resulted from the reaction of $Li_{0.53}(Ni_{0.8}Co_{0.15}Al_{0.05})O_2$ material with the possible products of the decomposition of PVDF (H_2, HF, C_xH_y…). The reducing gases, made of H_2 and HF gases from the decomposed binder, were likely the cause of the reduction of $Li_{0.53}(Ni_{0.8}Co_{0.15}Al_{0.05})O_2$ to form the NiO-type material. Furthermore, and under these conditions, HF gas can easily react with the lithium ions remaining in the charged active powder and form the LiF compound. In any cases, the mechanism by which the products of the decomposition of PVDF react with the $Li_{0.53}(Ni_{0.8}Co_{0.15}Al_{0.05})O_2$ powder needs to be identified.

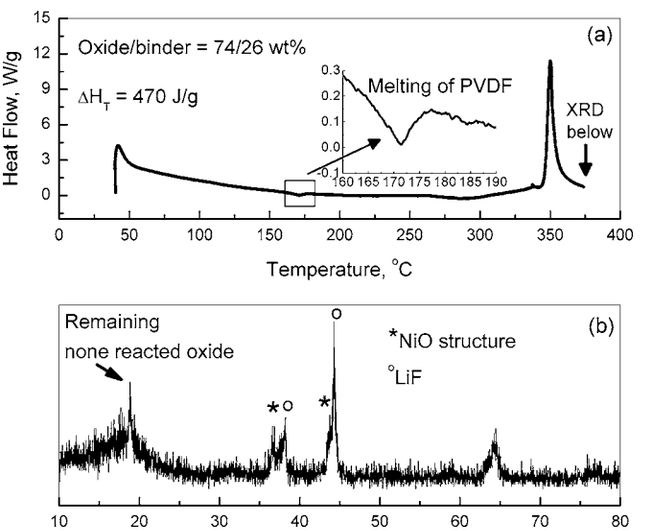

Figure 10. (a) DSC profiles of $Li_{0.53}(Ni_{0.8}Co_{0.15}Al_{0.05})O_2$ powder in the presence of PVDF solid binder, and (b) XRD pattern of the recovered sample after the DSC experiment.

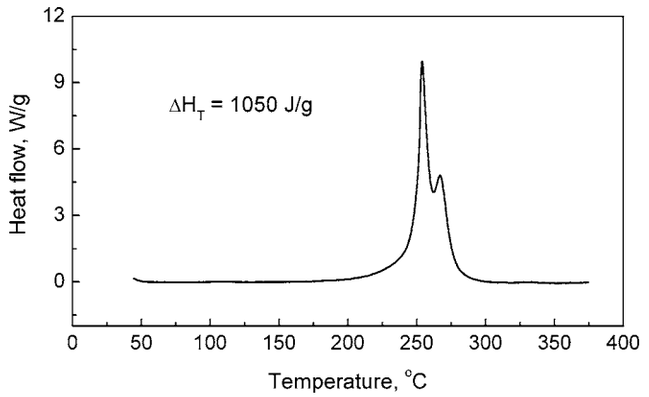

Figure 11. DSC curve of the electrode made of $Li_{0.53}(Ni_{0.8}Co_{0.15}Al_{0.05})O_2$, carbon, and PVDF binder in the presence of 1.2 M $LiPF_6$ (EC/EMC = 3:7 wt %) electrolyte.

Figure 11 shows the DSC plot of the electrode made of 84 wt % $Li(Ni_{0.8}Co_{0.15}Al_{0.05})O_2$, 8 wt % carbon, and 8 wt % PVDF that was charged to 4.2 V vs Li metal in the presence of 1.2 M $LiPF_6$ (EC/EMC = 3:7 wt %) electrolyte. In this case, the DSC thermal signatures and the amount of heat generated from the reaction between the charged $Li(Ni_{0.8}Co_{0.15}Al_{0.05})O_2$ electrode and the electrolyte were quite similar to those observed from the reaction between the same electrolyte and the charged powder $Li_{0.53}(Ni_{0.8}Co_{0.15}Al_{0.05})O_2$, as seen in Fig. 9. Furthermore, the amount of the heat generated from the reaction between the charged electrode and the electrolyte (1050 J/g) is very close to the heat generated from the reaction between the charged powder $Li_{0.53}(Ni_{0.8}Co_{0.15}Al_{0.05})O_2$ and the solvent (1150 J/g) (see Fig. 5b). In this case, the solvent concentration was 22 wt %, which is very close to the concentration of the electrolyte in the porous electrode (20 to ~25%). This result clearly shows that the contributions of the binder, carbon additive, and salt are negligible in the overall thermal heat resulting from the reaction between the positive electrode and the electrolyte. This also means that the main source of the exothermic heat after the thermal abuse of the cell is the reaction involving the oxidation of the solvent by the oxygen released from the decomposed charged positive active material, as reported by Maleki et al.[17] and Arai et al.[18]

Conclusion

Layered $Li_{0.53}(Ni_{0.8}Co_{0.15}Al_{0.05})O_2$ material was prepared from $Li(Ni_{0.8}Co_{0.15}Al_{0.05})O_2$ by charging the latter in a lithium cell without carbon and PVDF additives. The oxygen release from the $Li_{0.53}(Ni_{0.8}Co_{0.15}Al_{0.05})O_2$ powder resulted in its structural transformation from a layered ($R\bar{3}m$) to a NiO-type compound ($Fd3m$), as demonstrated by the TGA and XRD techniques. The thermal reactivity of the layered $Li_{0.53}(Ni_{0.8}Co_{0.15}Al_{0.05})O_2$ powder with several solvents, $LiPF_6$ salt, PVDF binder, and different nonaqueous electrolytes was investigated by the DSC technique. The results show that the contribution of the salt and binder in the overall thermal abuse of an electrode made of the $Li(Ni_{0.8}Co_{0.15}Al_{0.05})O_2$ positive active material is expected to be very limited in the generation of heat. When the $LiPF_6$ salt is dissolved in a solvent system to form an electrolyte, the reaction with the $Li_{0.53}(Ni_{0.8}Co_{0.15}Al_{0.05})O_2$ powder is delayed toward high temperature, if compared with the reaction that occurs between the powder and the solvents alone. In both cases, whether the exothermal reaction occurs at lower temperature (solvents) or high temperature (electrolytes), the heat generated is very similar. These results clearly show that one of the main sources for the thermal reactions in lithium-ion cells containing layered oxides such as $Li(Ni_{0.8}Co_{0.15}Al_{0.05})O_2$ is the oxidation of the solvents by the oxygen released by the unstable charged active oxides during thermal events. Therefore, there is at present no means to completely suppress the oxidation of the electrolyte with charged positive electrodes unless no-oxygen-release-type cathodes such as $LiFePO_4$ olivine are developed. At the moment and without sacrificing the energy and power characteristics of the lithium-ion cells, barriers towards developing stable layered oxides such as $Li(Ni_{1/3}Co_{1/3}Mn_{1/3})O_2$ and $LiNi_{1/2}Mn_{1/2}O_2$ electrode systems need to removed.

Acknowledgments

The authors acknowledge the financial support of the U.S. Department of Energy, FreedomCAR, and Vehicle Technologies Office, under contract no. W-31-109-Eng-38.

Argonne National Laboratory assisted in meeting the publication costs of this article.

References

1. E. P. Roth and D. H. Doughty, *J. Power Sources*, **128**, 308 (2004).
2. C. H. Chen, J. Liu, M. E. Stoll, G. Henriksen, D. R. Vissers, and K. Amine, *J. Power Sources*, **128**, 278 (2004).
3. D. P. Abraham, S. D. Poppen, A. N. Jansen, J. Liu, and D. W. Dees, *Electrochim. Acta*, **49**, 4763 (2004).
4. G. G. Botte, R. E. White, and Z. Zhang, *J. Power Sources*, **97-98**, 507 (2001).
5. D. D. MacNeil, T. D. Hatchard, and J. R. Dahn, *J. Electrochem. Soc.*, **148**, A663 (2001).
6. D. D. MacNeil and J. R. Dahn, *J. Electrochem. Soc.*, **149**, A912 (2002).
7. W. Lu, C. W. Lee, R. Venkatachalapathy, and J. Prakash, *J. Appl. Electrochem.*, **30**, 1119 (2000).
8. J. Rodriguez-Carvajal, in Abstracts of the Satellite Meeting on Powder Diffraction of the XV Congress of the IUCr, Toulouse, France, p. 127 (1990).
9. D. Taylor, *Br. Ceram. Trans. J.*, **83**, 5 (1984).
10. M. Yousuf, P.-C. Sahu, H.-K. Jajoo, S. Rajagopalan, and K. Rajan, *J. Phys. F: Met. Phys.*, **16**, 373 (1986).
11. M. Guilmard, L. Croguennec, D. Denux, and C. Delmas, *Chem. Mater.*, **15**, 4476 (2003).
12. M. Guilmard, L. Croguennec, and C. Delmas, *Chem. Mater.*, **15**, 4484 (2003).
13. S. Venkatraman, Y. Shin, and A. Manthiram, *Electrochem. Solid-State Lett.*, **6**, A9 (2003).
14. D. D. MacNeil and J. R. Dahn, *J. Electrochem. Soc.*, **150**, A21 (2003).
15. D. Aurbach, *J. Power Sources*, **89**, 206 (2000).
16. D. D. MacNeil and J. R. Dahn, *J. Electrochem. Soc.*, **148**, 1205 (2001).
17. H. Maleki, G. Deng, A. Anani, and J. Howard, *J. Electrochem. Soc.*, **146**, 3224 (1999).
18. H. Arai, M. Tsuda, K. Saito, M. Hayashi, and Y. Sakurai, *J. Electrochem. Soc.*, **149**, A401 (2002).